

Bore Reconstruction of Woodwind Instruments Using the Full Waveform Inversion

Augustin Ernout, Juliette Chabassier

► **To cite this version:**

Augustin Ernout, Juliette Chabassier. Bore Reconstruction of Woodwind Instruments Using the Full Waveform Inversion. e-Forum Acusticum, Dec 2020, Lyon / Virtual, France. hal-02996142

HAL Id: hal-02996142

<https://hal.inria.fr/hal-02996142>

Submitted on 9 Nov 2020

HAL is a multi-disciplinary open access archive for the deposit and dissemination of scientific research documents, whether they are published or not. The documents may come from teaching and research institutions in France or abroad, or from public or private research centers.

L'archive ouverte pluridisciplinaire **HAL**, est destinée au dépôt et à la diffusion de documents scientifiques de niveau recherche, publiés ou non, émanant des établissements d'enseignement et de recherche français ou étrangers, des laboratoires publics ou privés.

BORE RECONSTRUCTION OF WOODWIND INSTRUMENTS USING THE FULL WAVEFORM INVERSION

Augustin Ernoult, Juliette Chabassier

Magique-3D team, Inria Bordeaux Sud-Ouest, 200, avenue de la Vieille Tour, 33405 Talence, France

augustin.ernoult@inria.fr

ABSTRACT

Several techniques can be used to reconstruct the internal geometry of a wind instrument from acoustics measurements. In this study, the passive linear acoustic response of the instrument is simulated and an optimization process is used to fit the simulation to the measurements. This technique can be seen as a first step toward the design of wind instruments, where the targeted acoustics properties come no more longer from measurements but are imposed by the designer. The difficulties of this approach are to find the best acoustic observation allowing the reconstruction (impedance, reflection function, etc.) but also to have an efficient optimization process. The "full waveform inversion" (FWI) is a technique coming from the seismology community. It uses the knowledge of the equation modeling the wave propagation into the instrument (here the telegraphist equation) to have an explicit expression of the gradient of the function which is minimized. This gradient is evaluated with a low computational cost. The FWI methodology, along with 1D spectral finite element discretization in space, applied to the woodwind instruments (with tone holes, losses and radiation) is presented in this communication. The results obtained for the bore reconstruction with different acoustics observations are then compared and discussed.

1. INTRODUCTION

The aim of the bore reconstruction is to deduce the internal geometry of a wind instrument (bore profile) from acoustic measurement (typically input impedance measurement), giving a non-destructive tool to estimate the geometry of existing instrument.

Several previous studies conducted bore reconstruction of brass instruments, in which the resonator part is composed of one unique main tube, but to our knowledge, no reconstruction of woodwind instrument (with side holes) has been conducted. One approach is the pulse reflectometry technique [1, 2], a signal approach in which the main tube is supposed to be composed of small conical parts, the length of which are related to highest frequency of the signal. However this technique can not be applied directly to woodwind instruments in which the resonator can be seen as a "pipes network" due to the side holes. A second possibility is to use optimization algorithms to inverse the impedance computation: find the geometry which minimizes the residual between measured

and simulated impedance. This approach has been used by W.Kausel [3] on brass instruments by using a zero order optimization algorithm (Rosenbrock). This approach can be seen as a first step toward the design of wind instruments, where the targeted acoustics properties come no more longer from measurements but are imposed by the designer. Even if this principle can be applied to woodwind instruments, due to the complexity of the resonator geometry, it is necessary to use a more efficient optimization algorithm like quasi-Newton algorithm [4, Chap.3] for which the gradient of the objective function must be known.

The "full waveform inversion" (FWI) is a technique coming from the seismology community [5]. It uses the knowledge of the equation modeling the wave propagation to have an explicit expression of the gradient of the acoustic fields inside the propagation medium. It gives the possibility to evaluate, with a low computational cost, the gradient of the objective function of the optimization problem as long as its relation to the acoustic field is differentiable.

The general principle of the FWI and its adaptation to woodwind instrument reconstruction are first presented. The reconstruction of an illustrative "instrument" is then discussed: a cylindrical pipe with four side holes.

All the results presented in this paper are obtained using the OpenWInD python GPLv3 toolbox, the latest version of which can be downloaded at openwind.gitlabpages.inria.fr.

2. INVERSE PROBLEM

2.1 Wave propagation model

To solve the wave equation in the resonator of the instrument and compute its input impedance, it is described as a pipes network. The main bore profile can be described by one or several pipes with any shape (with axial symmetry). At the side holes location, a T-joint junction is assumed between the two pipes of the main bore and the cylindrical pipe corresponding to the chimney hole. The design parameters necessary to describe this geometry are grouped in the vector \mathbf{m} . The physical coefficients of the equations may therefore depend on \mathbf{m} .

In each pipe n the scaled telegraphist equation is as-

sumed:

$$\begin{cases} L_n(\mathbf{m})Z_v(x, \mathbf{m}, \omega)u_n + \frac{dp_n}{dx} = 0 \\ L_n(\mathbf{m})Y_t(x, \mathbf{m}, \omega)p_n + \frac{du_n}{dx} = 0 \end{cases} \quad \forall x \in [0, 1]. \quad (1)$$

where L_n is the pipe length, p_n is the acoustic pressure and u_n the acoustic flow. The coefficients Z_v and Y_t account for thermo-viscous effects and depend on the geometry:

$$\begin{cases} Z_v(x, \mathbf{m}, \omega) = \frac{j\omega\rho}{S(x)} [1 - \mathcal{J}(k_v(\mathbf{m}, \omega)R(x))]^{-1} \\ Y_t(x, \mathbf{m}, \omega) = \frac{j\omega S(x)}{\rho c^2} [1 + (\gamma - 1)\mathcal{J}(k_t(\mathbf{m}, \omega)R(x))] \end{cases}$$

$$k_v(\mathbf{m}, \omega) = \sqrt{j\omega\frac{\rho}{\mu}}, \quad k_t(\mathbf{m}, \omega) = \sqrt{j\omega\rho\frac{C_p}{\kappa}}$$

where R is the section radius, $S = \pi R^2$ is the section area, Table 1 describes the air constants and the function \mathcal{J} of a complex variable is defined as

$$\mathcal{J}(z) = \frac{2}{z} \frac{J_1(z)}{J_0(z)}, \quad \forall z \in \mathbb{C} \quad (3)$$

where J_0 and J_1 are the Bessel functions of the first kind [6].

Air density (kg.m ⁻³)	$\rho = 1.2929(T_0/(T + T_0))$
Sound celerity (m.s ⁻¹)	$c = 331.45\sqrt{(T + T_0)/T_0}$
Viscosity (kg.m ⁻¹ .s ⁻¹)	$\mu = 1.708e^{-5}(1 + 2.9e^{-3}T)$
Therm. cond. (Cal/(m.s.°C))	$\kappa = 5.77e^{-3}(1 + 3.3e^{-3}T)$
Specific heat (Cal/(kg. °C))	$C_p = 240$
Ratio of spec. heat	$\gamma = 1.402$

Table 1. Physical constant values [7]. T is the temperature in Celsius and $T_0 = 273.15\text{K}$. In this study $T = 20^\circ\text{C}$.

The boundary conditions of each pipe depend on its situation in the global instrument. At the entry (first point of the first pipe), a unitary input flow is imposed : $u_1(x = 0, \omega) = 1$. At the junctions between two main pipes (indexed by a and b) and one side hole (indexed by c), the entry flow is conserved and the entry pressures of each pipe follow a coupled equation [7, Chap.7]:

$$v_a + v_b + v_c = 0, \quad \begin{pmatrix} p_a - p_c \\ p_b - p_c \end{pmatrix} = \begin{pmatrix} m_{11} & m_{12} \\ m_{21} & m_{22} \end{pmatrix} j\omega \begin{pmatrix} v_a \\ v_b \end{pmatrix}$$

where the efficient masses can be obtained from measurements [7].

At each pipe end, a radiation impedance is imposed [8]:

$$(\alpha + j\omega\beta) p_n(1, \omega) = j\omega Z_c v_n(1, \omega) \quad (4)$$

where α and β are chosen to describe various radiation models, and can be put to $(0, 0)$ to model a closed hole.

For each pipe the equations are discretized by the Finite Element Method (FEM) leading to a linear matrix equation [9]. The junction and radiation equations are appended

in order to close the discrete system. This procedure results in a global matricial formulation for each considered frequency $f = \omega/2\pi$:

$$A_{tot}(\mathbf{m}, \omega)U_{tot} = E_{tot}. \quad (5)$$

where all the geometric coefficients contribute to the matrix A_{tot} , the vector U_{tot} contains the acoustic flow and pressure at each degree of freedom (dof) for all pipes and the vector E_{tot} the source term (associated with the input boundary condition).

The system is then solved by inverting the matrix A_{tot} . The input impedance is then the pressure at the dof corresponding to the entry of the instrument:

$$Z = \mathcal{R}U_{tot} \quad (6)$$

where \mathcal{R} is the projection matrix to the corresponding dof.

2.2 Choice of observable

The aim of the reconstruction is to determine the value of the parameters in the design vector \mathbf{m} by minimizing the residuals between an experimental observation and a simulated one. In our case, the measured data being the impedance, the observation must be a function of the impedance $O(Z)$. To allow the use of quasi-Newton algorithm, this function must be \mathcal{C}_1 . The identity, the modulus (as long as it is far from 0) and the phase are good candidates. The reflection function

$$R = \frac{Z - 1}{Z + 1} \quad (7)$$

and its modulus are also interesting. The phase of the reflection function is wrapped and can not be used directly [10]. The cost function J minimized by the optimization algorithm is:

$$J(\mathbf{m}) = \sum_{\omega} \frac{1}{2} |O(Z_{simu}(\omega)) - O(Z_{meas}(\omega))|^2 \quad (8)$$

with Z_{simu} and Z_{meas} , the simulated and measured impedances respectively.

To perform correctly the reconstruction, the chosen observation must ideally be such that the cost function only has one local minimum in the design space at the point corresponding to the actual geometry. The evolution of the cost functions relying of previously evoked observations along one axis of the design space (the position of the first hole) are represented on Figure 1, for a specific scenario. In this case, the reflection function appears to be the observation with the least local minima (and the impedance phase to a lesser extent). It is the observation chosen for this study.

2.3 Gradient computation

To perform the optimization with a quasi-Newton algorithm it is necessary to estimate the gradient of the cost function with respect to each design variable m_i . It is for this step that the approach used for the Full Waveform Inversion in geophysics is particularly interesting.

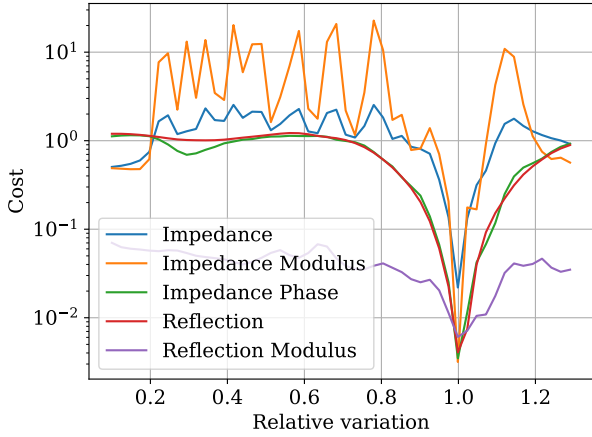


Figure 1. Variations of the residuals computed with different observations on the fingering where only the first hole is open, with respect to the relative location of the first hole. The reflection function has the smoother evolution.

The Frechet derivative is the mathematical framework used here. In some cases the adjoint state method can also be used efficiently [11].

The gradient of the cost function can easily be deduced from the differentiation of the acoustic fields with respect to the design variables $\partial U_{tot}/\partial m_i$, by formally using composed derivations with equations (6), (7) and (8).

The differentiation of the direct problem of Eq.(5) yields that the differentiation of the acoustic fields can be obtained by solving a similar problem with another source term:

$$A_{tot} \frac{\partial U_{tot}}{\partial m_i} = -\frac{\partial A_{tot}}{\partial m_i} U_{tot}. \quad (9)$$

This problem induces a low computational cost because the matrix A_{tot} is already to be inverted for the direct problem. The most technical part is maybe the computation of the derivative of A_{tot} which necessitates to differentiate the coefficients Z_v and Y_t .

3. RECONSTRUCTION OF AN ILLUSTRATIVE CASE

This reconstruction approach is here applied to a simple "woodwind-like" tube, the geometry of which is well known.

3.1 Description of the instrument

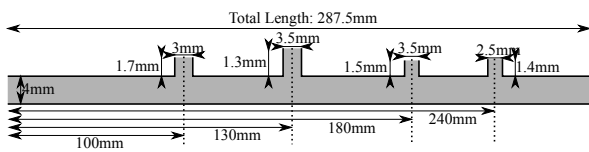


Figure 2. Sketch of the cylindrical tube with 4 side holes studied. It is described by 15 geometric parameters (3 for the main bore profile and 3 for each of the four holes).

The simple "woodwind-like" tube is a cylinder (treated here as a specific cone) drilled by four holes. The dimensions are indicated in Figure 2. In this study, only the main bore radius at the entrance is supposed known. The aim of the reconstruction is to determine the values of the 14 other parameters: the length and the right-end radius of the main pipe and the locations, the radii and the chimney heights of the four holes (14 unknowns).

A preliminary study reveals that the most useful "fingering" for the reconstruction are the ones for which at the most one hole is open. The 5 corresponding input impedances are measured.

3.2 Results

The initial geometry is a 5 cm conical pipe with one hole at each centimeter. A strategy is used to have a rough estimation of the geometry before refining the values of the design variables. For this first step, the low frequencies are the most important. Only 10 frequency values evenly spread between 100 Hz and 200 Hz. First of all the "all closed" impedance is used to adjust only the main bore profile (length and right-end radius). The impedance for which only the fourth hole is open is then used to adjust this hole location, and so on to adjust the four holes locations. These first optimizations are very fast (around 20 sec.), but due to the bad dimensions of the holes (radius and chimney heights) these first estimations of the locations are quite bad.

To refine the values, all the fingerings are taken into account and all the design variables are adjusted together. This time more frequencies are considered (100 values evenly spread between 100 Hz and 3000 Hz). This step is longer (around 5 min). The final results and the comparison with the measured geometric values are indicated in the tables 2, 3, 4, 5.

Variable	Measured	Reconstr.	Error
Total length	287.5 ± 0.5	287.57	0.07
Right-end diam.	4 ± 0.01	3.92	0.08

Table 2. Main bore dimensions (in mm): values obtained by geometric measurements and reconstruction.

Variable	Measured	Reconstr.	Error
Hole 1 loc.	100 ± 0.5	100.50	0.5
Hole 2 loc.	130 ± 0.5	130.46	0.46
Hole 3 loc.	180 ± 0.5	180.12	0.12
Hole 4 loc.	240 ± 0.5	240.18	0.18

Table 3. Holes locations (in mm): values obtained by geometric measurements and reconstruction.

It is important to notice that the measured locations have uncertainties around 0.5mm and the other dimensions around 0.01mm. The values obtained by the reconstruction process presented here are quite good for most of the design variables. At low frequency, the diameter and the chimney height of a hole have similar effect. The optimization algorithm can have difficulties to adjust together

Variable	Measured	Reconstr.	Error
Hole 1 diam.	3 ± 0.01	2.95	0.05
Hole 2 diam.	3.5 ± 0.01	3.54	0.04
Hole 3 diam.	3.5 ± 0.01	3.26	0.24
Hole 4 diam.	2.5 ± 0.01	2.19	0.31

Table 4. Holes diameters (in mm): values obtained by geometric measurements and reconstruction.

Variable	Measured	Reconstr.	Error
Chimney 1	1.7 ± 0.01	1.74	0.04
Chimney 2	1.3 ± 0.01	1.46	0.16
Chimney 3	1.5 ± 0.01	1.52	0.02
Chimney 4	1.4 ± 0.01	1.14	0.26

Table 5. Holes chimney heights (in mm): values obtained by geometric measurements and reconstruction.

these two parameters. It can explain the "wide" deviation between measured and reconstructed values for the dimension of the hole 4. Using higher frequencies could improve the reconstruction. The radiation model could also be a source of uncertainties in the reconstruction, since a model error should impact the way physical coefficients influence the simulated impedances, especially close to the holes open end.

Finally, the errors on the reconstruction can come from uncertainties on the input impedance measurement. The relative uncertainties on the input impedance of a cylinder are around 8% with the home-made sensor used for this study and built following the principles described by Gibiat [12] with five microphones. A preliminary study of the error propagation in the studied geometry gives around 1mm of uncertainty on the locations, 0.4mm on the diameters and 0.5mm on the chimney heights. It appears therefore that the major identified defect of the reconstruction process presented here is the precision of the impedance measurements.

4. CONCLUSION

This article presents the adaptation of the Full Waveform Inversion to the bore reconstruction of woodwind instrument (pipe with side holes). The process is applied to the reconstruction of a cylinder pipe with four side holes. The results indicate that the process is able to reconstruct such an instrument but that it is very sensitive to the precision of the measured impedance used for the reconstruction. Performing the inversion directly from the measured pressure at the five microphones instead of using post processed quantities (impedance, reflection function) could reduce these uncertainties by providing redundant data to the algorithm.

5. REFERENCES

- [1] D. B. Sharp, Acoustic pulse reflectometry for the measurement of musical wind instruments. PhD thesis, University of Edinburgh, 1996.
- [2] N. Amir, U. Shimony, and G. Rosenhouse, "A Discrete Model for Tubular Acoustic Systems with Varying Cross Section – The Direct and Inverse Problems. Part 1: Theory," Acta Acustica united with Acustica, vol. 81, pp. 450–462, Sept. 1995.
- [3] W. Kausel, "Optimization of Brasswind Instruments and its Application in Bore Reconstruction," Journal of New Music Research, vol. 30, pp. 69–82, Mar. 2001.
- [4] J. Nocedal and S. J. Wright, Numerical optimization. Springer series in operations research, New York: Springer, 2nd ed ed., 2006.
- [5] J. Virieux and S. Operto, "An overview of full-waveform inversion in exploration geophysics," GEOPHYSICS, vol. 74, pp. WCC1–WCC26, Nov. 2009.
- [6] H. Tijdeman, "On the propagation of sound waves in cylindrical tubes," Journal of Sound and Vibration, vol. 39, no. 1, pp. 1–33, 1975.
- [7] A. Chaigne and J. Kergomard, Acoustics of Musical Instruments. Modern Acoustics and Signal Processing, New York: Springer, 2016.
- [8] L. Rabiner and R. Schafer, Digital Processing of speech signals. 1978.
- [9] R. Tournemenne and J. Chabassier, "A comparison of a one-dimensional finite element method and the transfer matrix method for the computation of wind music instrument impedance," Acta Acustica united with Acustica, vol. 5, p. 838, 2019.
- [10] A. Ernout, C. Vergez, S. Missoum, P. Guillemain, and M. Jousserand, "Woodwind instrument design optimization based on impedance characteristics with geometric constraints." Mar. 2020.
- [11] R.-E. Plessix, "A review of the adjoint-state method for computing the gradient of a functional with geophysical applications," Geophysical Journal International, vol. 167, pp. 495–503, Nov. 2006.
- [12] V. Gibiat and F. Laloë, "Acoustical impedance measurements by the two-microphone-three-calibration (TMTTC) method," The Journal of the Acoustical Society of America, vol. 88, pp. 2533–2545, Dec. 1990.